



The structural modification of thiophene-linked porphyrin sensitizers for dye-sensitized solar cells

Na Xiang^a, Xianwei Huang^a, Xiaoming Feng^a, Yijiang Liu^a, Bin Zhao^{a,b}, Lijun Deng^a, Ping Shen^a, Junjie Fei^a, Songting Tan^{a,b,*}

^a College of Chemistry, Key Laboratory of Environmentally Friendly Chemistry and Applications of Ministry of Education, Xiangtan University, Xiangtan 411105, PR China

^b Key Laboratory of Advanced Functional Polymeric Materials of College of Hunan Province, Xiangtan University, Xiangtan 411105, PR China

ARTICLE INFO

Article history:

Received 17 March 2010

Received in revised form

7 May 2010

Accepted 7 May 2010

Available online 19 May 2010

Keywords:

Porphyrin derivative

Thiophene derivatives

π -Spacer unit

Incident photon-to-current conversion

efficiency

Dye-sensitized solar cells

Photovoltaic performances

ABSTRACT

Three donor–(π -spacer)–acceptor porphyrin dyes were synthesized for use in dye-sensitized solar cells. The dyes comprised the same donor (porphyrin derivative) and acceptor/anchoring group (2-cyanoacrylic acid) but varying π -spacer consisting of a combination of 4-methylthiophene, 4-hexylthiophene or 3,4-ethylenedioxythiophene groups. The dyes displayed different adsorption behavior and coverage of the TiO₂ surface.

© 2010 Elsevier Ltd. All rights reserved.

1. Introduction

In recent years, increasing demands for renewable energy sources have focused attention on the utilisation of solar energy. In this context, dye-sensitized solar cells (DSSCs) have attracted considerable interest owing to their ability to convert solar energy to electricity at low cost. In dye-sensitized solar cells, light is absorbed by a dye and charge separation takes place owing to photoinduced electron injection from the dye into the conduction band of TiO₂, the separated charges then move toward respective electrodes, thereby yielding a photocurrent in an external circuit [1]. To develop more efficient dyes for DSSCs, essential design requirements must be satisfied. Firstly, the sensitizing dyes must strongly adhere to the photocatalyst (TiO₂) surface to ensure efficient electron injection into the conduction band of TiO₂. Secondly, the lowest unoccupied molecular orbital (LUMO) of the dye must be sufficiently higher than the conduction band of TiO₂ for efficient charge

injection, and the highest occupied molecular orbital (HOMO) of the dye must be lower than the hole-transport material (HTM) for efficient regeneration of the oxidized dye. Finally, the dye must have light-harvesting ability in both the visible and/or near IR regions [2]. To date, the most efficient dye sensitizers employed in DSSCs are polypyridyl ruthenium complexes, with a solar-to-electricity conversion efficiency (η) of 10–11% [3]. The advantages of such ruthenium complexes are that they exhibit both broad absorption in the near-UV and visible region and appropriate excited-state oxidation potentials for the electron injection into TiO₂ [4]. However, these dyes are not readily available because of their high cost and the low availability of noble metals such as ruthenium.

Extensive researches have been devoted to the development of alternative, efficient metal-free dyes, which offer advantages as photosensitizers in that they have high molar absorption coefficients due to intramolecular π – π^* transitions and their structures can be modified easily and economically. In recent years, whilst various metal-free dyes based on coumarins [5], indolines [6], perylenes [7], merocyanines [8], porphyrins [9], triarylamines [10], and carbazoles [11] have been reported, such compounds display overall conversion efficiencies in the range 5–10%; however, the cell performances of metal-free dyes are either lower than or comparable to that of Ru dye-based DSSCs. Recently, porphyrins

* Corresponding author. College of Chemistry, Key Laboratory of Environmentally Friendly Chemistry and Applications of Ministry of Education, Xiangtan University, Xiangtan 411105, PR China.

E-mail address: tanst2008@163.com (S. Tan).

have been recognized as the most promising dyes for such application because of their photochemical and electrochemical stability, strong absorbing ability in the visible region due to π – π^* transitions of the conjugated macrocycle and high molar extinction coefficient [12]. However, the narrow absorption spectra of porphyrins, which poorly matches solar light distribution, limits the performance of porphyrin-sensitized solar cells. In order to solve this problem, many model compounds based on porphyrin have been synthesized for application in DSSCs. For example, Seunghun et al. synthesized β , β' -quinoxalino porphyrins containing carboxylic acid binding groups, which showed broadened and red-shifted light absorption band with the aid of π -extension; DSSCs based on the porphyrin dyes exhibited excellent power conversion efficiency of 5.2% [13]. Campbell et al. also have reported porphyrin dyes with extended π -systems by modifying a β -position with an olefinic linkage, which resulted in broad, red-shifted absorption bands; the dyes showed cell efficiency of 7.1% [14].

Despite major advances in porphyrin chemistry, further improvements in photovoltaic performance are needed. This paper concerns the use of a donor–(π -spacer)–acceptor (D– π –A) system for metal-free dyes intended for use in DSSCs, as means of securing effective photoinduced intramolecular charge transfer [10, 15]. In this work, a series of *meso*-position modified porphyrin sensitizers with porphyrin moieties as donors, thiophene derivatives as π -conjugated linkers, and cyanoacrylic acids as acceptors and anchoring groups (Fig. 1) were synthesized. The compounds were expected to have broader absorption than the corresponding porphyrin without thiophene cyanoacrylic acid groups, resulting in high short-circuit photocurrent (J_{sc}) and high solar-to-electricity conversion efficiency (η). Herein, three *meso*-4-methylphenyl groups were introduced to reduce the extent of aggregation occurring between neighboring porphyrins adsorbed on TiO₂ surface by means of steric hindrance. Different thiophene derivatives employed as π -linkers for connecting the porphyrin donors (D) and anchor (A) groups, not only extended the light absorption region but also affected the electron injection character of the dyes into the TiO₂ surface.

The introduction of 3,4-ethylenedioxythiophene (EDOT) into the porphyrin dye was anticipated to enhance photovoltaic performance because EDOT has a small torsional angle with the adjoining phenyl fragment, thereby ensures efficient electronic transfer between D and A. The effects of the different π -conjugated linkers on the photophysical, electrochemical properties and photovoltaic performances were investigated.

2. Experimental

2.1. Materials and reagents

All starting materials were purchased from Pacific ChemSource and Alfa Aesar. DMF, CHCl₃, CH₃CN and POCl₃ were dried and distilled by accustomed methods before use. All other solvents and chemicals used in this work were analytical grade and used without further purification. All chromatographic separations were carried out on silica gel (200–300 mesh).

2.2. Analytical measurements

¹H and ¹³C NMR spectra were recorded with a Bruker Avance 400 instrument. UV–vis spectra of the dyes were measured on a Perkin–Elmer Lamada 25 spectrometer. The PL spectra were obtained using Perkin–Elmer LS-50 luminescence spectrometer. MALDI-TOF mass spectrometric measurements were performed on Bruker Biflex III MALDI-TOF. Electrochemical redox potentials were obtained by cyclic voltammetry (CV) and differential pulse voltammetry (DPV) using a three-electrode configuration and an electrochemistry workstation (CHI660A, Chenhua Shanghai). The working electrode was a glassy carbon electrode; the auxiliary electrode was a Pt electrode, and saturated calomel electrode (SCE) was used as reference electrode. Tetrabutylammonium perchlorate (TBAP) 0.1 M was used as supporting electrolyte in dry DMF. Ferrocene was added to each sample solution at the end of the experiments, and was used as an internal potential reference [16].

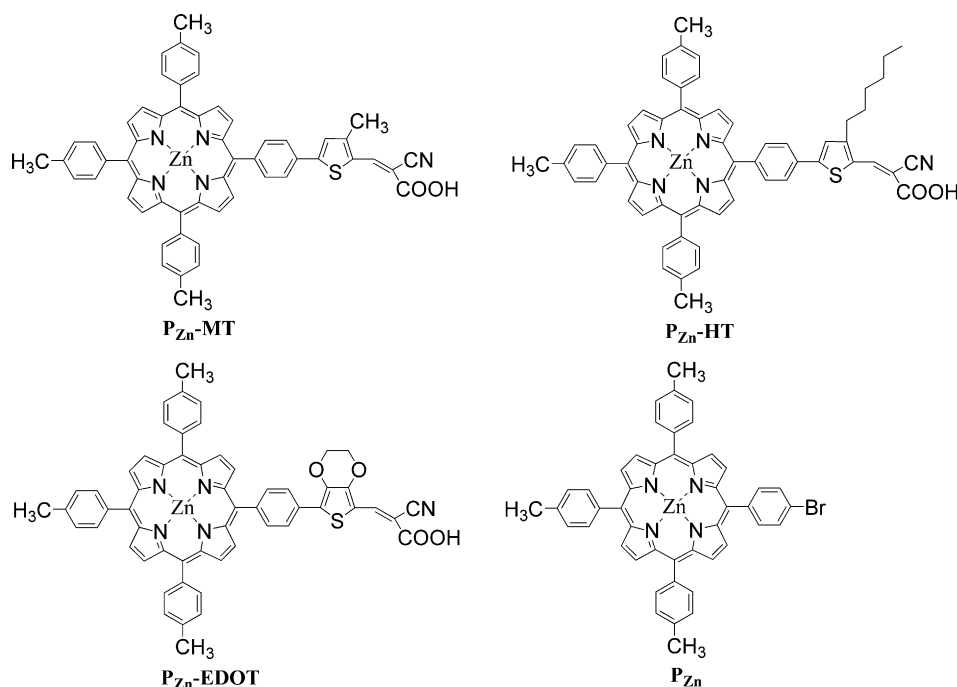


Fig. 1. Molecular structures of porphyrin derivatives used in this study.

2.3. General procedure for preparation and test of solar cells

Fluorine-doped SnO₂ conducting glass (FTO) was immersed in aqueous 40 mM TiCl₄ solution at 70 °C for 30 min, washed with water and ethanol and then sintered at 450 °C for 30 min. 20–30 nm particle size TiO₂ colloid blended with 0.1% magnesium acetate solution was applied to the FTO glass using a sliding glass rod to obtain a TiO₂ film of 10–15 μm thickness after drying. 200 nm particle size TiO₂ colloid was applied to the electrode using the same method, resulting in a TiO₂ light-scattering layer of 4–6 μm thickness. The TiO₂ electrodes were immersed in a 1 mM DMF solution of the porphyrin dyes at room temperature. After dye adsorption, the dye-coated TiO₂ electrodes were copiously rinsed with ethanol.

Photovoltaic measurements were performed in a sandwich cell consisting of the porphyrin dye-sensitized TiO₂ electrode as the working electrode and a Pt foil as counter electrode. The electrolyte comprised 0.5 M LiI, 0.05 M I₂, and 0.5 M 4-*tert*-butylpyridine (TBP) in 3-methoxypropionitrile and the irradiated area of the cell was 0.196 cm². The photocurrent–voltage (*J*–*V*) characteristics were measured with a Keithley 2602 Source meter under 100 mW cm⁻² irradiation using a 500 W Xe lamp with a global AM 1.5 filter for solar spectrum simulation. The solar-to-electricity conversion efficiency (η) of the DSSCs was calculated from the short-circuit photocurrent density (*J*_{sc}), the open-circuit photovoltage (*V*_{oc}), the fill factor (*FF*) and the intensity of the incident light (*P*_{in}) according to the following equation:

$$\eta = \frac{J_{sc}(\text{mA cm}^{-2}) \times V_{oc}(\text{V}) \times FF}{P_{in}(\text{mW cm}^{-2})}$$

The IPCE values were plotted as a function of the excited wavelength and defined according to the following equation:

$$\text{IPCE}(\lambda) = \frac{1240}{\lambda(\text{nm})} \times \frac{J_{sc}(\text{mA cm}^{-2})}{\Phi(\text{mW cm}^{-2})}$$

where *J*_{sc} is the short-circuit photocurrent density generated by monochromatic light, λ is the wavelength of incident monochromatic light, and Φ is the incident light intensity.

2.4. Synthesis

The synthetic routes to the three porphyrin dyes are shown in Fig. 2. The detailed synthetic procedures were as follows.

2.4.1. 2-(*Tri-n-butylstannyl*)-4-methyl thiophene (**1**)

Under an argon atmosphere, 3-methyl thiophene (1.96 g, 20 mmol) and 50 mL freshly distilled dry THF were placed in a 100 mL three-necked flask. *n*-Butyllithium (8.8 mL, 2.5 mol L⁻¹ in hexane, 22 mmol) was added dropwise at –78 °C, and the solution was stirred at –78 °C for 1 h. Tributyltin chloride (6 mL, 22 mmol) was then added and the mixture was allowed to reach room temperature slowly and stirred for another 24 h. Finally, the mixture was poured into 100 mL of cooled water and extracted by hexane. The organic layer was dried over anhydrous MgSO₄. Removal of the solvent by rotary evaporation yielded a yellow–brown liquid **1** (6.98 g, 90%). The crude product was used in next step without further purification. ¹H NMR (CDCl₃, 400 MHz, ppm): 7.19 (s, 1 H thienyl-H), 6.97 (s, 1 H, thienyl-H), 2.30 (s, 3 H, –CH₃), 1.53 (m, 6 H, –CH₂–), 1.34 (m, 6 H, –CH₂–), 1.11 (m, 6 H, –CH₂–), 0.88 (m, 9 H, –CH₃).

2.4.2. 2-(*Tri-n-butylstannyl*)-4-hexyl thiophene (**2**)

The synthetic procedure for **2** was similar to that for **1**, except that 3-hexyl thiophene (3.36 g, 20 mmol) was used instead of

3-methyl thiophene. A yellow–brown liquid **2** (8.25 g, 90%) was obtained. The crude product was used in next step without further purification. ¹H NMR (CDCl₃, 400 MHz, ppm): 7.18 (s, 1 H, thienyl-H), 6.96 (s, 1 H, thienyl-H), 2.64 (t, 2 H, –CH₂–), 1.62–1.54 (m, 8 H, –CH₂–), 1.36–1.30 (m, 12 H, –CH₂–), 1.11–1.06 (m, 6 H, –CH₂–), 0.93–0.87 (m, 12 H, –CH₃).

2.4.3. 4-(4-Methyl)thienyl benzaldehyde (**3**)

4-Bromobenzaldehyde (1.84 g, 10 mmol) and **1** (3.88 g, 10 mmol) were dissolved in 100 mL of DMF, and the mixture was purged with nitrogen for 30 min. Pd (PPh₃)₄ (115 mg, 0.1 mmol) was then added after stirring at 100 °C for 24 h, the ensuing mixture was poured into 100 mL of cooled water and extracted by chloroform. The organic layer was dried over anhydrous MgSO₄. Removal of the solvent was carried out by rotary evaporation and the crude product was purified using silica chromatography employing petroleum ether/dichloromethane = 1/1 to give **3** as a yellow solid (1.62 g, 80%). ¹H NMR (CDCl₃, 400 MHz, ppm): 10.11 (s, 1 H, CHO–H), 8.02 (d, 2 H, phenyl-H), 7.86 (d, 2 H, phenyl-H), 7.38 (s, 1 H, thienyl-H), 7.09 (s, 1 H, thienyl-H), 2.50 (s, 3 H, CH₃–). ¹³C NMR (CDCl₃, ppm): 188.14, 139.05, 138.17, 137.46, 137.03, 129.75, 128.44, 124.73, 120.50, 19.01.

2.4.4. 4-(4-Hexyl)thienyl benzaldehyde (**4**)

The synthetic procedure was similar to that described for **3**, except that **2** (4.58 g, 10 mmol) was used instead of **1**. The crude product was purified on a silica chromatograph with petroleum ether/dichloromethane = 2/1 to give **4** as a yellow solid (2.31 g, 85%). ¹H NMR (CDCl₃, 400 MHz, ppm): 9.98 (s, 1 H, CHO–H), 7.88 (d, 2 H, phenyl-H), 7.72 (d, 2 H, phenyl-H), 7.24 (s, 1 H, thienyl-H), 6.95 (s, 1 H, thienyl-H), 2.53 (t, 2 H, –CH₂–), 1.62 (t, 2 H, –CH₂–), 1.23 (m, 6 H, –CH₂–), 0.96 (t, 3 H, CH₃–). ¹³C NMR (CDCl₃, ppm): 191.34, 139.75, 138.43, 138.10, 137.15, 130.67, 128.01, 125.56, 122.07, 32.14, 31.87, 31.44, 29.26, 22.78, 14.15.

2.4.5. 5-(4-(4-Methyl)thienyl)phenyl-10,15,20-tris(4-methylphenyl) porphyrin (**5**)

In a 500 mL three-necked flask, 4-methylbenzaldehyde (3.06 g, 25.5 mmol) and **3** (1.71 g, 8.5 mmol) were dissolved in 300 mL propionic acid. The solution was heated to reflux at 140 °C. Pyrrole (2.28 g, 34 mmol) was then added dropwise and the mixture stirred for another 30 min. After cooling to room temperature, half of the solvent was evaporated and 150 mL CH₃OH was added. The mixture was cooled over night and filtered under vacuum. The crude product was purified using column chromatography (petroleum ether/dichloromethane = 2/3 as an eluent). After recrystallization from the mixture of CHCl₃ and CH₃OH (1:5, v/v), a desired purple solid of compound **5** was obtained (1.60 g, 25%). ¹H NMR (CDCl₃, 400 MHz, ppm): 8.97 (m, 8 H, pyrrolic-H), 8.21 (d, 2 H, phenyl-H), 8.10 (d, 6 H, phenyl-H), 7.96 (d, 2 H, phenyl-H), 7.55 (d, 6 H, phenyl-H), 7.42 (s, 1 H, thienyl-H), 6.99 (s, 1 H, thienyl-H), 2.70 (s, 9 H, –CH₃), 2.39 (s, 3 H, –CH₃), –2.11 (s, 2 H, N–H). MALDI-TOF MS calcd for C₅₂H₄₀N₄S 752.30; found 751.94.

2.4.6. 5-(4-(4-Hexyl)thienyl)phenyl-10,15,20-tris(4-methylphenyl) porphyrin (**6**)

The synthetic procedure for **6** was similar to that recounted for **5**, except that **4** (2.31 g, 8.5 mmol) was used instead of **3**. The crude product was purified using silica chromatograph with dichloromethane to give **6** as a purple solid (1.68 g, 24%). ¹H NMR (CDCl₃, 400 MHz, ppm): 8.97 (m, 8 H, pyrrolic-H), 8.21 (d, 2 H, phenyl-H), 8.10 (d, 6 H, phenyl-H), 7.96 (d, 2 H, phenyl-H), 7.55 (d, 6 H, phenyl-H), 7.47 (s, 1 H, thienyl-H), 7.01 (s, 1 H, thienyl-H), 2.70 (s, 9 H, –CH₃), 2.53 (t, 2 H, –CH₂–), 1.62 (t, 2 H, –CH₂–), 1.23 (m, 6 H, –CH₂–), 0.96 (t, 3 H, CH₃–), –2.11 (s, 2 H, N–H). MALDI-TOF MS calcd for C₅₇H₅₀N₄S 822.38; found 822.59.

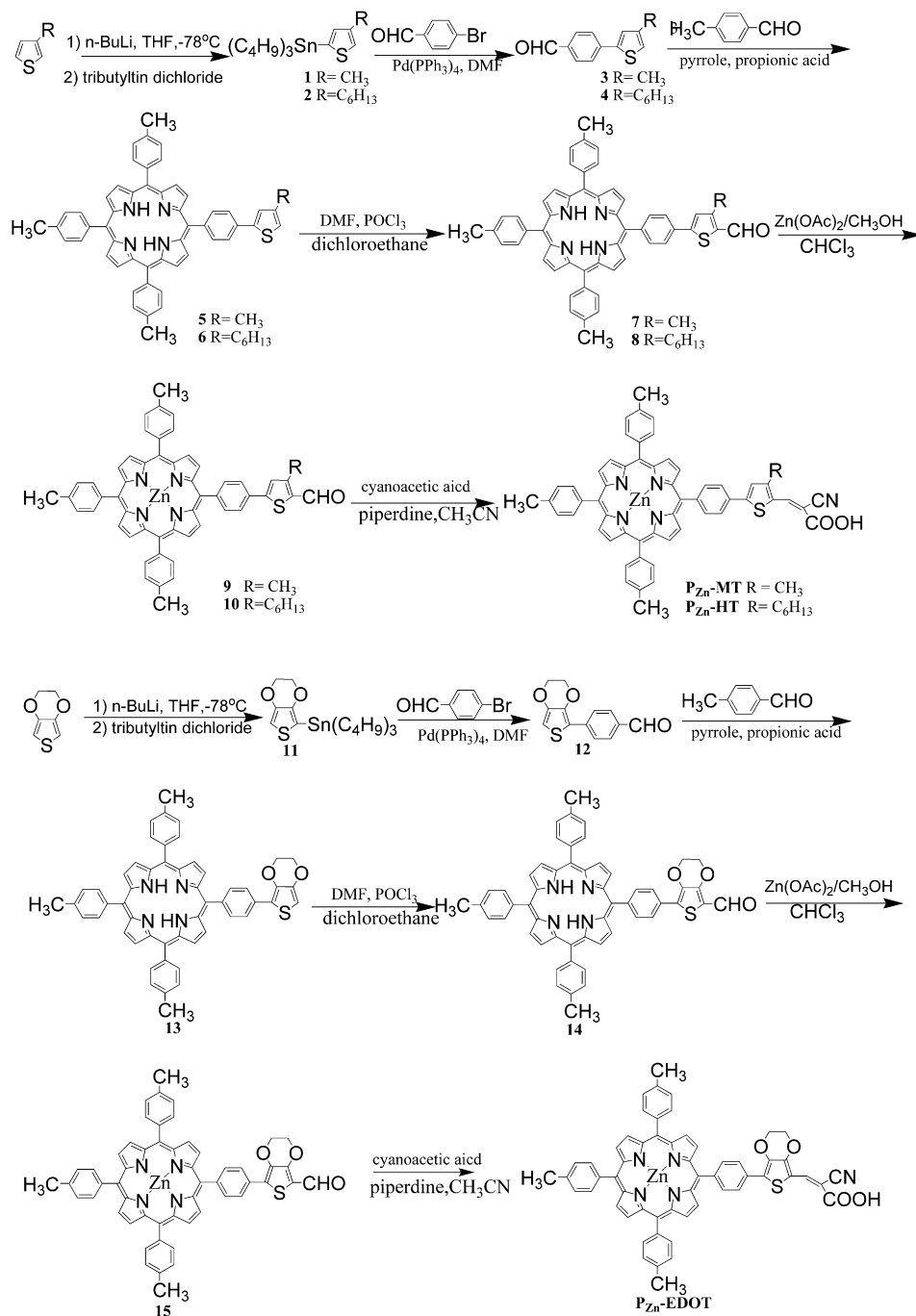


Fig. 2. Synthesis of porphyrin dyes.

2.4.7. 5-(4-(4-Methyl-5-formyl)thienyl)phenyl-10,15,20-tris(4-methylphenyl)porphyrin (7)

In a 100 mL three-necked flask, DMF (2.0 mL, 24 mmol) and POCl_3 (2.2 mL, 24 mmol) were added in turn at 0°C under nitrogen. After stirring for 5 min, **5** (0.9 g, 1.2 mmol) was added and the reaction mixture was refluxed for 12 h and then was stirred at room temperature for 1.5 h after which it was poured into sodium acetate solution (40 mL). The mixture was extracted with dichloromethane, and the extract was washed with water and dried over anhydrous MgSO_4 . The solvent was evaporated, and the residue was purified by column chromatography on silica gel with petroleum ether/dichloromethane = 1/2, a purple solid of compound **7** was obtained

(0.37 g, 40%). ^1H NMR (CDCl_3 , 400 MHz, ppm): 10.16 (s, 1 H, CHO-H), 8.89 (m, 8 H, pyrrolic-H), 8.28 (d, 2 H, phenyl-H), 8.13 (d, 6 H, phenyl-H), 8.07 (d, 2 H, phenyl-H), 7.59 (d, 6 H, phenyl-H), 7.52 (s, 1 H, thienyl-H), 2.73 (s, 12 H, $-\text{CH}_3$), -2.33 (s, 2 H, N-H). MALDI-TOF MS calcd for $\text{C}_{53}\text{H}_{40}\text{N}_4\text{OS}$ 780.29; found 779.74.

2.4.8. 5-(4-(4-Hexyl-5-formyl)thienyl)phenyl-10,15,20-tris(4-methylphenyl)porphyrin (8)

The synthetic procedure for **8** was similar to that described for **7**, except that **6** (1.0 g, 1.2 mmol) was used instead of **5**. The crude product was purified on a silica chromatograph with petroleum ether/dichloromethane = 1/1 to give **8** as a purple solid (0.49 g,

48%). ^1H NMR (CDCl_3 , 400 MHz, ppm): 10.13 (s, 1 H, CHO), 8.88 (m, 8 H, pyrrolic-H), 8.28 (d, 2 H, phenyl-H), 8.10 (d, 6 H, phenyl-H), 8.04 (d, 2 H, phenyl-H), 7.57 (d, 6 H, phenyl-H), 7.52 (s, 1 H, thienyl-H), 3.08 (t, 2 H, $-\text{CH}_2-$), 2.70 (s, 9 H, $-\text{CH}_3$), 1.62 (t, 2 H, $-\text{CH}_2-$), 1.23 (m, 6 H, $-\text{CH}_2-$), 0.96 (t, 3 H, CH_3-), -2.11 (s, 2 H, N-H). MALDI-TOF MS calcd for $\text{C}_{58}\text{H}_{50}\text{N}_4\text{O}_5\text{S}$ 850.37; found 850.58.

2.4.9. 5-(4-(4-Methyl-5-formyl)thienyl)phenyl-10,15,20-tris(4-methylphenyl)porphyrin Zinc (**9**)

In a 250 mL one-necked round-bottomed flask, a mixture of **7** (0.39 g, 0.5 mmol) and Zn(OAc) $_2$ (0.92 g, 5 mmol) in a solution of CHCl_3 (100 mL) and CH_3OH (10 mL) was refluxed for 4 h. After cooling to room temperature, the mixture was washed with water. The organic layer was dried over anhydrous MgSO_4 and concentrated. A purple-red solid of compound **9** was obtained (0.41 g, 97%). ^1H NMR (CDCl_3 , 400 MHz, ppm): 10.13 (s, 1 H, CHO), 8.88 (m, 8 H, pyrrolic-H), 8.28 (d, 2 H, phenyl-H), 8.10 (d, 6 H, phenyl-H), 8.04 (d, 2 H, phenyl-H), 7.57 (d, 6 H, phenyl-H), 7.48 (s, 1 H, thienyl-H), 2.70 (s, 12 H, $-\text{CH}_3$). MALDI-TOF MS calcd for $\text{C}_{53}\text{H}_{38}\text{N}_4\text{O}_5\text{Zn}$ 842.21; found 842.47.

2.4.10. -(4-(4-Hexyl-5-formyl)thienyl)phenyl-10,15,20-tris(4-methylphenyl)porphyrin Zinc (**10**)

The synthetic procedure for **10** was similar to that described for **9**, except that **8** (0.42 g, 0.5 mmol) was used instead of **7**. A purple-red solid of compound **10** was obtained (0.43 g, 95%). ^1H NMR (CDCl_3 , 400 MHz, ppm): 10.13 (s, 1 H, CHO), 8.88 (m, 8 H, pyrrolic-H), 8.28 (d, 2 H, phenyl-H), 8.10 (d, 6 H, phenyl-H), 8.04 (d, 2 H, phenyl-H), 7.57 (d, 6 H, phenyl-H), 7.52 (s, 1 H, thienyl-H), 3.08 (t, 2 H, $-\text{CH}_2-$), 2.70 (s, 9 H, $-\text{CH}_3$), 1.62 (t, 2 H, $-\text{CH}_2-$), 1.23 (m, 6 H, $-\text{CH}_2-$), 0.96 (t, 3 H, CH_3-). MALDI-TOF MS calcd for $\text{C}_{58}\text{H}_{48}\text{N}_4\text{O}_5\text{Zn}$ 912.28; found 912.35.

2.4.11. 2-Cyano-3-(3-methyl-5-(4-(10,15,20-tris(4-methylphenyl)porphyrinatozinc(II)yl)phenyl)thienyl acrylic acid (**P_{Zn}-MT**)

A 50 mL acetonitrile solution of **9** (0.29 g, 0.34 mmol) and cyanoacetic acid (0.06 g, 0.68 mmol) was refluxed in the presence of 0.3 mL piperidine for 8 h under a nitrogen atmosphere. After cooling to room temperature, the reaction mixture was poured into a mixture of distilled water and 2.0 M HCl and then extracted with chloroform. The organic layer was washed with water and dried over anhydrous MgSO_4 . After the removal of solvent, the crude product was purified by column chromatography over silica gel with a dichloromethane/methanol mixture (10:1) yielding the product as a purple solid **P_{Zn}-MT** (0.20 g, 65%). ^1H NMR (CDCl_3 , 400 MHz, ppm): 8.91 (m, 8 H, pyrrolic-H), 8.29 (d, 2 H, phenyl-H), 8.22 (d, 2 H, phenyl-H), 8.15 (d, 6 H, phenyl-H), 7.85 (s, 1 H, vinyl-H), 7.55 (d, 6 H, phenyl-H), 7.43 (s, 1 H, thienyl-H), 2.70 (s, 12 H, $-\text{CH}_3$). ^{13}C NMR (CDCl_3 , ppm): 162.4, 150.0, 149.9, 149.5, 140.3, 137.1, 135.7, 134.6, 132.3, 132.1, 131.8, 129.8, 128.4, 127.7, 124.6, 121.0, 120.9, 119.3, 115.7, 21.5, 15.0. MALDI-TOF MS calcd for $\text{C}_{56}\text{H}_{39}\text{N}_5\text{O}_2\text{S}_2\text{Zn}$ 909.21; found 909.18.

2.4.12. 2-Cyano-3-(3-hexyl-5-(4-(10,15,20-tris(4-methylphenyl)porphyrinatozinc(II)yl)phenyl)thienyl acrylic acid (**P_{Zn}-HT**)

The synthetic procedure for **P_{Zn}-HT** was similar to that described for **P_{Zn}-MT**, except that **10** (0.31 g, 0.34 mmol) was used instead of **9**. A purple solid of compound **P_{Zn}-HT** was obtained (0.19 g, 58%). ^1H NMR (CDCl_3 , 400 MHz, ppm): 8.95 (m, 8 H, pyrrolic-H), 8.32 (d, 2 H, phenyl-H), 8.27 (d, 2 H, phenyl-H), 8.18 (d, 6 H, phenyl-H), 7.89 (s, 1 H, vinyl-H), 7.56 (d, 6 H, phenyl-H), 7.46 (s, 1 H, thienyl-H), 3.08 (t, 2 H, $-\text{CH}_2-$), 2.70 (s, 9 H, $-\text{CH}_3$), 1.62 (t, 2 H, $-\text{CH}_2-$), 1.23 (m, 6 H, $-\text{CH}_2-$), 0.96 (t, 3 H, CH_3-). ^{13}C NMR (CDCl_3 , ppm): 161.9, 150.0, 149.9, 149.5, 144.2, 140.3, 137.1, 135.6, 134.5, 132.3, 132.1, 131.8, 127.7, 127.6, 124.6, 120.9, 119.5, 31.6, 31.1, 28.9,

22.6, 21.5, 14.5. MALDI-TOF MS calcd for $\text{C}_{61}\text{H}_{49}\text{N}_5\text{O}_2\text{S}_2\text{Zn}$ 979.29; found 979.28.

2.4.13. 2-(Tri-*n*-butylstannyl)-3,4-ethylenedioxythiophene (**11**)

The synthetic procedure for **11** was similar to that recounted above for **1**, except that 3,4-ethylene dioxy thiophene (2.84 g, 20 mmol) was used instead of 3-methyl thiophene. A yellow-brown liquid **11** (6.91 g, 80%) was obtained. ^1H NMR (CDCl_3 , 400 MHz, ppm): 6.57 (s, 1 H thienyl-H), 4.13 (d, 4 H, $-\text{OCH}_2$), 1.53 (m, 6 H, $-\text{CH}_2$), 1.34 (m, 6 H, $-\text{CH}_2$), 1.11 (m, 6 H, $-\text{CH}_2$), 0.88 (m, 9 H, $-\text{CH}_3$).

2.4.14. 4-(3,4-Ethylene dioxy)thienyl benzaldehyde (**12**)

The synthetic procedure for **12** was similar to that described for **3**, except that **11** (4.58 g, 10 mmol) was used instead of **1**. The crude product was purified on a silica chromatograph with petroleum ether/dichloromethane = 1/1 to give **12** as a yellow solid (2.09 g, 85%). ^1H NMR (CDCl_3 , 400 MHz, ppm): 9.97 (s, 1 H, CHO-H), 7.87 (m, 4 H, phenyl-H), 6.42 (s, 1 H, thienyl-H), 4.43 (m, 2 H, $-\text{OCH}_2$), 4.28 (m, 2 H, OCH_2). ^{13}C NMR (CDCl_3 , 100 MHz, ppm): 190.08, 152.45, 139.64, 136.93, 130.37, 127.75, 114.30, 94.92, 65.33.

2.4.15. 5-(4-(3,4-Ethylenedioxy)thienyl)phenyl-10,15,20-tris(4-methylphenyl) porphyrin (**13**)

The synthetic procedure for **13** was similar to that recounted for **5**, except that **12** (2.09 g, 8.5 mmol) was used instead of **3**. The crude product was purified on a silica chromatograph with dichloromethane to give **13** as a purple solid (1.68 g, 25%). ^1H NMR (CDCl_3 , 400 MHz, ppm): 8.97 (m, 8 H, pyrrolic-H), 8.21 (d, 2 H, phenyl-H), 8.10 (d, 8 H, phenyl-H), 7.55 (d, 6 H, phenyl-H), 6.39 (s, 1 H, thienyl-H), 4.43 (d, 2 H, $-\text{OCH}_2$), 4.32 (d, 2 H, $-\text{OCH}_2$), 2.71 (s, 9 H, $-\text{CH}_3$), -2.01 (s, 2 H, N-H). MALDI-TOF MS calcd for $\text{C}_{53}\text{H}_{40}\text{N}_4\text{O}_2\text{S}$ 796.29; found 796.50.

2.4.16. 5-(4-(3,4-Ethylenedioxy-5-formyl)thienyl)phenyl-10,15,20-tris(4-methylphenyl) porphyrin (**14**)

The synthetic procedure for **14** was similar to that described for **7**, except that **13** (0.95 g, 1.2 mmol) was used instead of **5**. The crude product was purified on a silica chromatograph with petroleum ether/dichloromethane = 1/2 to give **14** as a purple solid (0.42 g, 42%). ^1H NMR (CDCl_3 , 400 MHz, ppm): 10.05 (s, 1 H, CHO-H), 8.85 (m, 8 H, pyrrolic-H), 8.27 (d, 2 H, phenyl-H), 8.20 (d, 2 H, phenyl-H), 8.18 (d, 6 H, phenyl-H), 7.57 (d, 6 H, phenyl-H), 4.53 (s, 4 H, $-\text{OCH}_2$), 2.70 (s, 9 H, CH_3), -2.75 (s, 2 H, N-H). MALDI-TOF MS calcd for $\text{C}_{54}\text{H}_{40}\text{N}_4\text{O}_3\text{S}$ 824.28; found 824.73.

2.4.17. 5-(4-(3,4-Ethylenedioxy-5-formyl)thienyl)phenyl-10,15,20-tris(4-methylphenyl) porphyrin Zinc (**15**)

The synthetic procedure for **15** was similar to that described for **9**, except that **14** (0.41 g, 0.5 mmol) was used instead of **7**. A purple-red solid of compound **15** was obtained (0.43 g, 97%). ^1H NMR (CDCl_3 , 400 MHz, ppm): 10.05 (s, 1 H, CHO), 8.85 (s, 8 H, pyrrolic-H), 8.27 (d, 2 H, phenyl-H), 8.20 (d, 2 H, phenyl-H), 8.18 (d, 6 H, phenyl-H), 7.57 (d, 6 H, phenyl-H), 4.53 (s, 4 H, $-\text{OCH}_2$), 2.70 (s, 9 H, CH_3). MALDI-TOF MS calcd for $\text{C}_{54}\text{H}_{38}\text{N}_4\text{O}_3\text{S}_2\text{Zn}$ 886.20; found 885.93.

2.4.18. 2-Cyano-3-(3,4-ethylenedioxy-5-(4-(10,15,20-tris(4-methylphenyl)porphyrinatozinc(II)yl)phenyl)thienyl acrylic acid (**P_{Zn}-EDOT**)

The synthetic procedure for **P_{Zn}-EDOT** was similar to that described for **P_{Zn}-MT**, except that **15** (0.30 g, 0.34 mmol) was used instead of **9**. A purple solid of compound **P_{Zn}-EDOT** was obtained (0.19 g, 58%). ^1H NMR (CDCl_3 , 400 MHz, ppm): 8.95 (s, 8 H, pyrrolic-H), 8.33 (d, 2 H, phenyl-H), 8.27 (d, 2 H, phenyl-H), 8.20 (d, 6 H, phenyl-H), 7.90 (s, 1 H, vinyl-H), 7.57 (d, 6 H, phenyl-H), 4.53 (s, 4 H, $-\text{OCH}_2$), 2.70 (s, 9 H, CH_3). ^{13}C NMR (CDCl_3 , ppm): 161.9, 150.0,

149.9, 149.5, 143.5, 140.3, 139.3, 137.1, 135.5, 134.5, 132.3, 132.0, 131.8, 130.9, 129.8, 127.7, 125.0, 121.0, 120.9, 119.6, 119.3, 115.7, 110.3, 21.5. MALDI-TOF MS calcd for $C_{57}H_{39}N_5O_4SZn$ 953.20; found 953.17.

3. Results and discussion

3.1. Synthesis and chemical characterization

All the dyes have been synthesized according to several classical reactions. The synthetic strategy is shown in Fig. 2. Taking 2-cyano-3-(3-methyl-5-(4-(10,15,20-tris(4-methylphenyl))porphyrinatozinc(II)yl)phenyl)thienyl acrylic acid (P_{Zn} -MT) as an example, the dye was synthesized as following steps. First, the starting material, 2-(tri-*n*-butylstannyl)-4-methyl thiophene **1**, was obtained from 3-methyl thiophene in the presence of *n*-BuLi and tributyltin chloride. Then the key intermediate **5** was obtained by two steps: (1) 4-(4-methyl)thienyl benzaldehyde **3** was synthesized by Stille coupling with 4-bromobenzaldehyde and compound **1**; (2) the compound **3** reacted with 4-methylbenzaldehyde and pyrrole to obtain compound **5**. Subsequently, compound **5** was converted into 5-(4-(4-methyl-5-formyl)thienyl)-phenyl-10,15,20-tris(4-methylphenyl)porphyrin **7** by Vilsmeier formylation with $POCl_3$ and DMF in 1,2-dichloroethane. Finally, compound **7** was treated with $Zn(OAc)_2$, and then reacted with cyanoacetic acid by Knoevenagel reaction to give P_{Zn} -MT. P_{Zn} -HT and P_{Zn} -EDOT were synthesized by the same procedure as that for P_{Zn} -MT except 4-hexyl thienyl or 3,4-ethylenedioxy thienyl group was used instead of 4-methyl thienyl group respectively. The structures of the three dyes were verified by 1H NMR, ^{13}C NMR, and MOLDI-TOF mass spectra.

3.2. Optical and electrochemical properties

The UV–vis absorption spectra of P_{Zn} , P_{Zn} -MT, P_{Zn} -HT and P_{Zn} -EDOT in $CHCl_3$ solution are shown in Fig. 3a, and the peak positions and molar absorption coefficients (ϵ) of Soret and Q bands of porphyrin dyes are listed in Table 1. The UV–vis absorption spectra of P_{Zn} exhibits a typical strong Soret band at 420 nm and moderate Q bands at 547 nm. However, as a result of expansion of the π -system by introducing thiophene units, the Soret bands (422–423 nm) and the Q bands (550 nm) of three porphyrin dyes are both broadened and slightly red-shifted compared with those of P_{Zn} . The molar extinction coefficients (ϵ) of Soret bands are $1.21 \times 10^5 \text{ mol L}^{-1} \text{ cm}^{-1}$ for P_{Zn} -MT, $2.02 \times 10^5 \text{ mol L}^{-1} \text{ cm}^{-1}$ for P_{Zn} -HT, and $2.55 \times 10^5 \text{ mol L}^{-1} \text{ cm}^{-1}$ for P_{Zn} -EDOT, respectively, all of which are much higher than that of $Ru(dcbpy)_2(NCS)_2$ (N3 dye: ca. $1.6 \times 10^4 \text{ mol L}^{-1} \text{ cm}^{-1}$) [17]. As seen from Fig. 3b, the absorption spectra of the three porphyrin dyes adsorbed onto TiO_2 films are similar to those of the corresponding solution spectra, but obviously red-shifted and broadening due to the formation of the J-type aggregates of porphyrins on the TiO_2 surface [18]. Additionally, the absorption band of P_{Zn} -EDOT is broader and slightly red-shifted in comparison with those of P_{Zn} -MT and P_{Zn} -HT, which should be attributed to a more extensive conjugation of molecules containing the EDOT moiety. It is indicated that P_{Zn} -EDOT has an enhanced ability to harvest solar light.

The kinetics of adsorption of the three porphyrin dyes on TiO_2 films were measured to study the procedure of porphyrin derivatives adsorbed onto the TiO_2 surface. Fig. 4 shows the curves obtained plotting values of absorbance at 560 nm for different times of sensitization. The three kinds of kinetics seem to be biphasic, which indicates that the dyes form multilayers on the TiO_2 surface. P_{Zn} -MT and P_{Zn} -EDOT have about the same kinetics and maximum absorbance with 0.6, and P_{Zn} -HT has a slower kinetic compared to the other two dyes with a smaller value of maximum

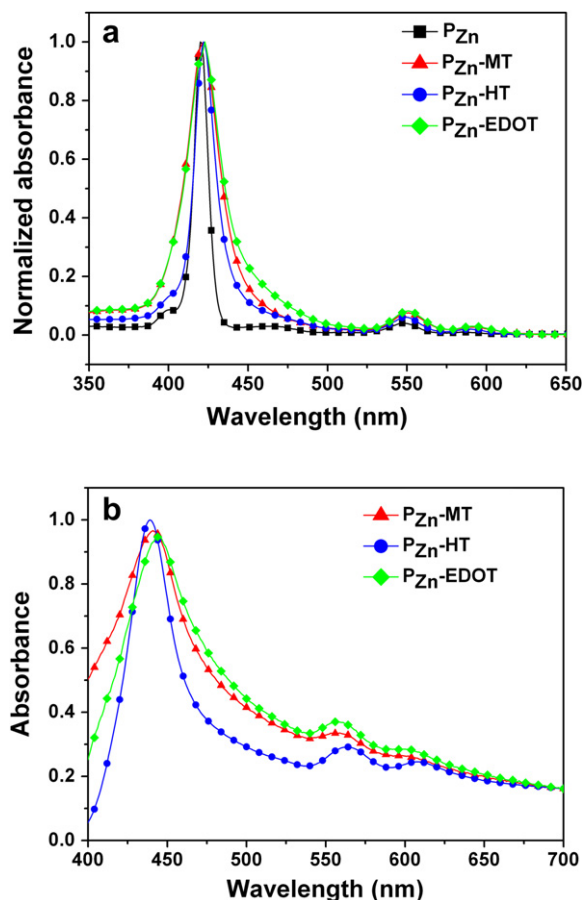


Fig. 3. UV–Vis absorption spectra of porphyrins in $CHCl_3$ solution (a) and TiO_2 films (b).

absorbance. This result is attributed to the introduction of a long hexyl chain into the thiophene segment for P_{Zn} -HT, which result in the decreasing of the absorption rate and the absorbed amounts of the dye onto the TiO_2 .

The strength of intermolecular interaction for porphyrin dyes, which may influence the solar cell performance, can be evaluated by means of the adsorbed dye amounts. The total amounts of the porphyrin dyes adsorbed on the TiO_2 films were determined by measuring the absorbance of the dyes, which were dissolved from the dye-coated TiO_2 films into $DMF/H_2O = 4:1$ with 0.1 mol L^{-1} NaOH. The surface density (Γ) values of the porphyrins absorption in DMF are listed in Table 1. The adsorbed amounts of P_{Zn} -MT ($1.8 \times 10^{-8} \text{ mol cm}^{-2}$) and P_{Zn} -EDOT ($1.3 \times 10^{-8} \text{ mol cm}^{-2}$) are larger than that of P_{Zn} -HT ($2.3 \times 10^{-9} \text{ mol cm}^{-2}$). These results

Table 1
UV, PL spectral data of porphyrin dyes.

dye	λ_{abs} ($\epsilon, 10^5 \text{ mol L}^{-1} \text{ cm}^{-1}$) ^a	Soret/ Q-band (f) ^b	Amount ^c / $10^{-8} \text{ mol cm}^{-2}$	λ_{em} (nm) ^d	λ_{int} (nm) ^e
P_{Zn} -MT	422(1.21),550(0.08)	441/559	1.8	608, 648	569
P_{Zn} -HT	422(2.02),550(0.16)	438/565	0.23	603, 646	563
P_{Zn} -EDOT	423(2.55),550(0.17)	453/567	1.3	609, 654	572
P_{Zn}	420(2.21),547(0.07)			598, 645	448

^a Absorption spectra was measured in $CHCl_3$ solution.

^b Absorption spectra was obtained on TiO_2 film.

^c Amount of the dyes adsorbed on TiO_2 film.

^d Wavelengths for emission spectra in $CHCl_3$ solution by exciting at Soret wavelength.

^e Measured by the intercept of the normalized absorption and emission spectra.

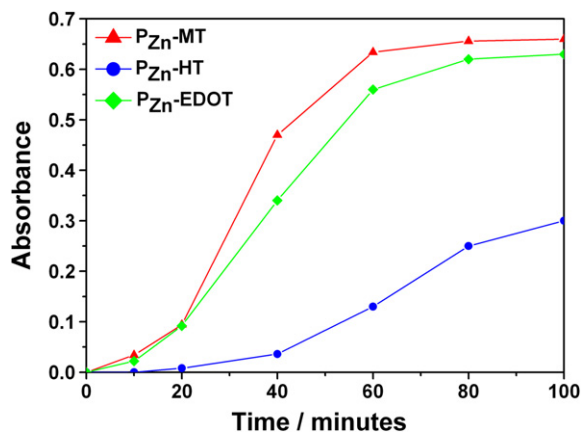


Fig. 4. Kinetics of adsorption of the three porphyrin dyes on TiO_2 films at 560 nm.

indicate that the porphyrin dyes with shorter alkyl or alkoxy chains have stronger intermolecular interaction than those with longer alkyl chains on the TiO_2 surface. In addition, the smaller molecular sizes of **PZn-MT** and **PZn-EDOT** are also responsible for the large adsorbed amount. As for **PZn-HT**, the hexyl chain linked to the π -conjugated segment of thiophene, which acts as a spacer to decrease intermolecular π - π interaction, thus reduced the adsorbed dye amount of **PZn-HT** [19].

The steady-state fluorescence spectra of **PZn**, **PZn-MT**, **PZn-HT** and **PZn-EDOT** were measured in CHCl_3 by exciting at the peak position of the Soret band (Fig. 5), and the emission maxima are summarized in Table 1. The emission maxima of **PZn-MT** (608 nm, 648 nm), **PZn-HT** (603 nm, 646 nm) and **PZn-EDOT** (609 nm, 654 nm) are red-shifted with respect to those of **PZn** (598 nm, 645 nm), which is consistent with the results of the UV–vis absorption spectra. No emission spectra were observed for the porphyrin dyes on TiO_2 film, which indicated that electron injection from the excited singlet state of the dyes into the conduction band of the TiO_2 completely [20]. From the intercept of the normalized UV–vis absorption spectra and steady-state fluorescence spectra, the zeroth–zeroth energies (E_{0-0}) are determined to be 2.18 eV for **PZn-MT**, 2.20 eV for **PZn-HT**, and 2.17 eV for **PZn-EDOT**, which are smaller than that of **PZn** (2.77 eV). These results indicate that the HOMO–LUMO gaps of the thiophene-linked porphyrin dyes are lower compared with that of **PZn** as a result of the extension of π system.

The redox potentials of the porphyrin dyes were obtained by cyclic voltammetry and differential pulse voltammetry. The results

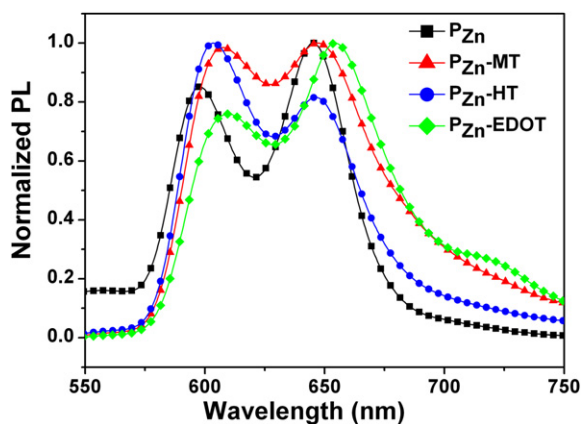


Fig. 5. PL spectra of **PZn**, **PZn-MT**, **PZn-HT** and **PZn-EDOT** in CHCl_3 .

Table 2
Electrochemical data for porphyrin dyes and driving forces for electron-transfer processes on the TiO_2 .

Dye	E_{0-0}^a (eV)	E_{ox}^b (V)	E_{red}^c (V)	E_{ox}^{*d} (V)	ΔG_{inj}^e (eV)	ΔG_{reg}^f (eV)
PZn-MT	2.18	0.968	−1.106	−1.212	−0.712	−0.468
PZn-HT	2.20	1.015	−1.097	−1.185	−0.685	−0.515
PZn-EDOT	2.17	0.950	−1.129	−1.220	−0.720	−0.450
PZn	2.77	1.230	−1.290	−1.540		

^a Determined from the intercept of the normalized absorption and emission spectra.

^b First oxidation potentials (vs NHE).

^c First reduction potentials (vs NHE).

^d Excited-state oxidation potentials approximated from E_{ox} and E_{00} (vs NHE).

^e Driving forces for electron injection from the porphyrin excited singlet state (E_{ox}^*) to the conduction band of TiO_2 (−0.5 V vs NHE).

^f Driving forces for regeneration of the porphyrin radical cation by I^-/I_3^- redox couple (+0.5 V vs NHE).

are summarized in Table 1. All porphyrins dyes show quasi-reversible waves for a one-electron oxidation and reduction. The oxidation potentials of **PZn-MT**, **PZn-HT** and **PZn-EDOT** ranging from 0.95 to 1.015 V vs NHE are negative relatively than that of **PZn** (1.23 V vs NHE). Moreover, the oxidation potential of dye **PZn-EDOT** (0.950 V) is slightly negative than those of **PZn-MT** (0.968 V) and **PZn-HT** (1.015 V) likely because the former has a strong electron-donating EDOT moiety. The first reduction potentials of **PZn-MT** (−1.106 V vs NHE), **PZn-HT** (−1.097 V vs NHE) and **PZn-EDOT** (−1.129 V vs NHE) are also positively shifted in comparison with **PZn** (−1.19 V vs NHE). Totally, the HOMO–LUMO gaps of **PZn-MT** (2.074 eV), **PZn-HT** (2.202 eV) and **PZn-EDOT** (2.079 eV) are smaller than that of **PZn** (2.52 eV), which is consistent with the aforementioned trend for the zeroth–zeroth energies. The result indicates that the introduction of thiophene derivatives could decrease the electrochemical gaps of porphyrin dyes. Meanwhile, from the UV–vis and PL spectra and electrochemical measurements, the driving forces for electron injection from the excited porphyrin singlet state to the conduction band (CB) of TiO_2 (−0.5 V vs NHE) (ΔG_{inj}) and the regeneration of porphyrin radical cation by I^-/I_3^- couple (0.5 V vs NHE) [21] (ΔG_{reg}) for the porphyrin-sensitized TiO_2 cells were determined and the corresponding data listed in Table 2. Both of the processes are thermodynamically feasible.

3.3. Photovoltaic properties of porphyrin-sensitized TiO_2 solar cells

In the dye-sensitized solar cells, the prepared method of TiO_2 electrode plays a key role. We used the double-layer TiO_2 film

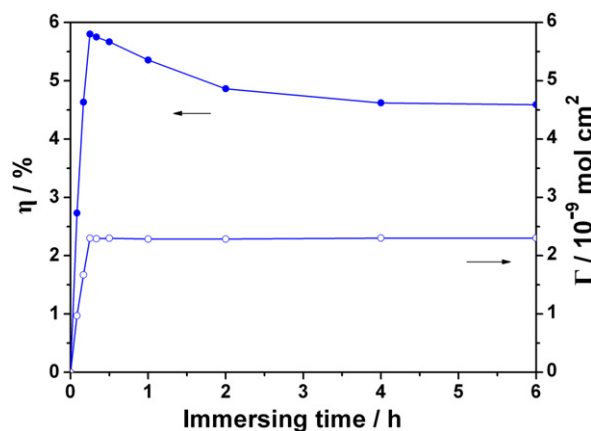


Fig. 6. Immersing time profiles of the η value (close circle) and the surface density (Γ) of the **PZn-HT** dye adsorbed on a TiO_2 electrode (open circle) in DMF.

Table 3
Photovoltaic performance of DSSCs for the three dyes.

Dye	J_{sc} (mA/cm ²)	V_{oc} (V)	FF	η (%)
P_{Zn}-MT	12.83	0.64	0.68	5.55
P_{Zn}-HT	13.71	0.63	0.67	5.80
P_{Zn}-EDOT	15.59	0.64	0.65	6.47

containing 20 nm and 200 nm TiO₂ particles as the photoanode to improve the ability of light harvesting. In addition, the performances of the porphyrin-sensitized TiO₂ solar cells are strongly affected by the solvents, immersing time and illuminating time. To optimize the condition of the dye baths of the porphyrin sensitizer for DSSCs, taking **P_{Zn}-HT** as an example, DMF, C₂H₅OH, CH₃CN, CHCl₃ were employed in DSSCs. The best η of 5.80% ($J_{sc} = 13.71 \text{ mA cm}^{-2}$, $V_{oc} = 0.63 \text{ V}$, and $FF = 0.67$) was obtained in DMF, which can be attributed to the higher dye density on the TiO₂ surface in DMF. To further improve the performance of the porphyrin-sensitized TiO₂ solar cells, the dependence of immersing time on the Γ and the η values for **P_{Zn}-HT** was measured in DMF. From the Fig. 6, it can be seen that the Γ values are increased rapidly with increasing the immersing time until it becomes saturated ($2.3 \times 10^{-9} \text{ mol cm}^{-2}$). In accordance with the initial trend of Γ , the η values are also enhanced with increase of the immersing time, but then the η values decrease gradually with further increase of the immersing time. Similar behavior was reported for many other porphyrin dyes [22]. The reasons may be associated with the change in orientation of the porphyrin molecules on the TiO₂ surface and/or in the binding strength to the TiO₂ surface [22b]. Furthermore, the dependence of the illuminating time on the η values for **P_{Zn}-HT** was also measured in DMF. The η values are increased rapidly in the first 30 min, and then increased slowly until the balance at 70 min. Similar results of **P_{Zn}-MT** and **P_{Zn}-EDOT** absorbed on TiO₂ electrode in DMF were obtained.

Table 3 summarizes the photovoltaic performance of the porphyrin-sensitized TiO₂ cells under the optimized conditions which the dyes were immersed in DMF for 15 min and illuminated for 70 min. The current-voltage characteristics of **P_{Zn}-MT**-, **P_{Zn}-HT**- and **P_{Zn}-EDOT** sensitized TiO₂ cells are shown in Fig. 7. **P_{Zn}-MT** sensitized cell exhibits $\eta = 5.55\%$ with $J_{sc} = 12.83 \text{ mA cm}^{-2}$, $V_{oc} = 0.64 \text{ V}$, and $ff = 0.68$, while **P_{Zn}-HT** sensitized one shows a higher $\eta = 5.80\%$ with $J_{sc} = 13.71 \text{ mA cm}^{-2}$, $V_{oc} = 0.63 \text{ V}$, and $ff = 0.67$, and **P_{Zn}-EDOT** sensitized one yields the highest $\eta = 6.47\%$ with $J_{sc} = 15.59 \text{ mA cm}^{-2}$, $V_{oc} = 0.64 \text{ V}$, and $ff = 0.65$. To a large extent, the three porphyrin dyes display rather similar V_{oc} and ff values. The different η values of the three porphyrin-sensitized

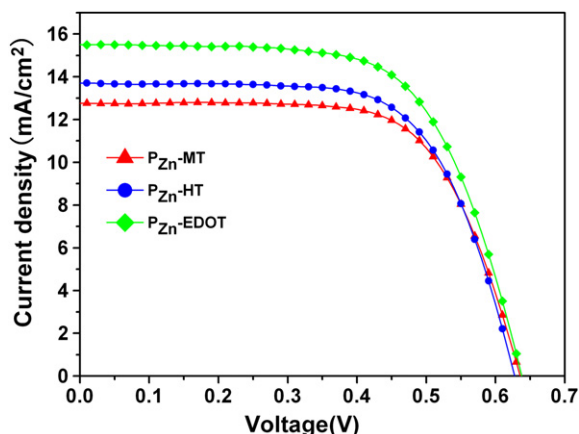


Fig. 7. Current density-voltage characteristics for DSSCs based on the three dyes.

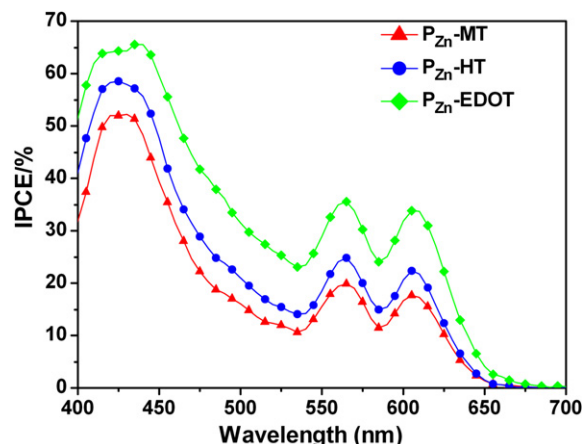


Fig. 8. IPCE plots for the DSSCs based on the three porphyrin dyes.

solar cells primarily result from the difference of J_{sc} . Because the Γ value of the dye-sensitized TiO₂ films is an important factor to determine the photocurrent generation. From Tables 1 and 3, we can see that the low J_{sc} of the **P_{Zn}-HT** sensitized TiO₂ cell compared to that of the **P_{Zn}-EDOT** sensitized cells mainly results from the low Γ value of TiO₂/**P_{Zn}-HT**. However, the highest Γ value of TiO₂/**P_{Zn}-MT** result in the lowest J_{sc} and η , which implies that too much dyes absorbed on TiO₂ film produce negative effect due to serious aggregation formation. It seems that the higher electron collection efficiency of **P_{Zn}-EDOT** determined by the moderate Γ value ($1.3 \times 10^{-8} \text{ mol cm}^{-2}$) is suitable for preparing high efficient DSSCs.

The differences in the η values among the porphyrin dyes can also be explained from incident photon-to-current conversion efficiency (IPCE) of three porphyrin-sensitized solar cells (Fig. 8). The shapes of these spectra are slightly broader but clearly follow the shape of the corresponding absorption spectra shown in Fig. 3b. The maximum IPCE_{max} value of **P_{Zn}-EDOT** (65%) is higher than both of **P_{Zn}-MT** (52%) and **P_{Zn}-HT** (58%), which is consistent well with the trend of η values. At longer wavelength region (gt; 500 nm), **P_{Zn}-EDOT** also displays higher IPCE values than those of **P_{Zn}-MT** and **P_{Zn}-HT**. These results are in good agreement with the photo-voltaic behavior of porphyrin-sensitized TiO₂ cells. Given the similar driving forces of three porphyrin dyes, the influence of electron injection efficiency in the η values is excluded. Therefore, the enhanced light-harvesting ability and higher electron collection efficiency of **P_{Zn}-EDOT** probably lead to the higher η value than those of **P_{Zn}-MT** and **P_{Zn}-HT**.

4. Conclusions

In summary, we have successfully synthesized three modified thiophene-linked porphyrin sensitizers (**P_{Zn}-MT**, **P_{Zn}-HT** and **P_{Zn}-EDOT**) in which porphyrin unit act as electron-donating moiety and cyanoacrylic acid as electron-accepting moiety bridged by MT, HT, and EDOT, respectively. By introducing the electron-rich EDOT moiety, the light absorption of **P_{Zn}-EDOT** has been broadened and slightly red-shifted compared to those of **P_{Zn}-MT** and **P_{Zn}-HT**. Therefore, **P_{Zn}-EDOT** exhibits the maximum power conversion efficiency of 6.47% with $J_{sc} = 15.59 \text{ mA cm}^{-2}$, $V_{oc} = 0.64 \text{ V}$ and $FF = 0.65$. Since electron injection efficiencies of the three porphyrin dyes are more or less similar, the light-harvesting ability and electron collection efficiencies of porphyrin sensitizers have strong influence on the photovoltaic performances. Our results demonstrate the necessity and importance of modifying π -spacers in D- π -A structure of porphyrin dyes. Inspired by the natural

light-harvesting ability of porphyrin derivatives, further structural modification of *meso*-substituted porphyrin for broadening the spectral absorption is anticipated to give some new porphyrin dyes with even better performances.

Acknowledgements

This work was supported by the National Nature Science Foundation of China (Project Nos. 50973092) and key project of Hunan Province of China (Project No. 2008FJ2004) and Nature Science Foundation of Hunan Province of China (09JJ3020, 09JJ4005). The authors are grateful to John N. Clifford and Emilio Palomares at Institute of Chemical Research of Catalonia (ICIQ) in Spain, for measuring the kinetics of adsorption of the porphyrin dyes on TiO₂ films.

References

- [1] (a) Wang Q, Campbell WM, Bonfantani EE, Jolley KW, Officer DL, Walsh PJ, et al. Efficient light harvesting by using green Zn-porphyrin-sensitized nanocrystalline TiO₂ films. *Journal of Physical Chemistry B* 2005;109:15397–409; (b) Hagfeldt A, Grätzel M. Molecular photovoltaics. *Accounts of Chemical Research* 2000;33:269–77; (c) Grätzel M. Solar energy conversion by dye-sensitized photovoltaic cells. *Inorganic Chemistry* 2005;44:6841–51.
- [2] (a) Robertson N. Optimizing dyes for dye-sensitized solar cells. *Angewandte Chemie International Edition* 2006;45:2338–45; (b) Tachibana Y, Haque SA, Mercer IP, Durrant JR, Klug DR. Electron injection and recombination in dye sensitized nanocrystalline titanium dioxide films: a comparison of ruthenium bipyridyl and porphyrin sensitizer dyes. *Journal of Physical Chemistry B* 2000;104:1198–205.
- [3] (a) Nazeeruddin MK, Angelis DF, Fantacci S, Selloni A, Viscardi G, Liska P, et al. Combined experimental and DFT-TDDFT computational study of photoelectrochemical cell ruthenium sensitizers. *Journal of American Chemical Society* 2005;127:16835–47; (b) Wang P, Klein C, Moser JE, Baker RH, Ha NLC, Charvet R, et al. Amphiphilic ruthenium sensitizer with 4,4'-diphosphonic acid-2,2'-bipyridine as anchoring ligand for nanocrystalline dye sensitized solar cells. *Journal of Physical Chemistry B* 2004;108:17553–9.
- [4] Grätzel M. Dye-sensitized solar cells. *Journal of Photochemistry and Photobiology C: Photochemistry Reviews* 2003;4:145–53.
- [5] (a) Wang ZS, Cui Y, Hara K, Dan-oh Y, Kasada C, Shinpo A. A high-light-harvesting-efficiency coumarin dye for stable dye-sensitized solar cells. *Advanced Materials* 2007;19:1138–41; (b) Hara K, Kurashige M, Danoh Y, Kasada C, Shinpo A, Suga S, et al. Design of new coumarin dyes having thiophene moieties for highly efficient organic-dye-sensitized solar cells. *New Journal of Chemistry* 2003;27:783–5.
- [6] Liu B, Zhu W, Zhang Q, Wu W, Xu M, Ning Z, et al. Conveniently synthesized isophorone dyes for high efficiency dye-sensitized solar cells: tuning photovoltaic performance by structural modification of donor group in donor- π -acceptor system. *Chemical Communications* 2009;13:1766–8.
- [7] Zafer C, Kus M, Turkmen G, Dincalp H, Demic S, Kuban B, et al. New perylene derivative dyes for dye-sensitized solar cells. *Solar Energy Materials and Solar Cells* 2007;91:427–31.
- [8] Ma X, Hua J, Wu W, Jin Y, Meng F, Zhan W, et al. A high-efficiency cyanine dye for dye-sensitized solar cells. *Tetrahedron* 2008;64:345–50.
- [9] Hayashi S, Tanaka M, Hayashi H, Eu S, Umeyama T, Matano Y, et al. Naphthyl-fused π -elongated porphyrins for dye-sensitized TiO₂ cells. *Journal of Physical Chemistry C* 2008;112:15576–85.
- [10] (a) Zhang G, Bala H, Cheng Y, Shi D, Lv X, Yu Q, et al. High efficiency and stable dye-sensitized solar cells with an organic chromophore featuring a binary π -conjugated spacer. *Chemical Communications* 2009;16:2198–200; (b) Xu W, Peng B, Chen J, Liang M, Cai F. New triphenylamine-based dyes for dye-sensitized solar cells. *Journal of Physical Chemistry C* 2008;112:874–80; (c) Shen P, Liu Y, Huang X, Zhao B, Xiang N, Fei J, et al. Efficient triphenylamine dyes for solar cells: effects of alkyl-substituents and π -conjugated thiophene unit. *Dyes and Pigments* 2009;83:187–97.
- [11] (a) Zhang XH, Wang ZS, Cui Y, Koumura N, Furube A, Hara K. Organic sensitizers based on hexylthiophene-functionalized Indolo[3,2-*b*]carbazole for efficient dye-sensitized solar cells. *Journal of Physical Chemistry C* 2009;113:13409–15; (b) Liu D, Zhao B, Shen P, Huang H, Liu L, Tan ST. Molecular design of organic dyes based on vinylene hexylthiophene bridge for dye-sensitized solar cells. *Science in China Series B: Chemistry* 2009;52:1198–209.
- [12] (a) Krebs FC, Hagemann O, Spanggaard H. Directional synthesis of a dye-linked conducting homopolymer. *The Journal of Organic Chemistry* 2003;68:2463–6; (b) Yamada H, Imahori H, Nishimura Y, Yamazaki I, Ahn TK, Kim SK, et al. Photovoltaic properties of self-assembled monolayers of porphyrins and porphyrin–fullerene dyads on ITO and gold surfaces. *Journal of the American Chemical Society* 2003;125:9129–39; (c) Hasobe T, Saito K, Kamat PV, Troiani V, Qiu H, Solladie N, et al. Organic solar cells. Supramolecular composites of porphyrins and fullerenes organized by polypeptide structures as light harvesters. *Journal of Materials Chemistry* 2007;17:4160–70; (d) Liu Y, Xiang N, Feng X, Shen P, Zhou W, Weng C, et al. Thiophene-linked porphyrin derivatives for dye-sensitized solar cells. *Chemical Communications* 2009;18:12499–501.
- [13] Eu S, Hayashi S, Umeyama T, Matano Y, Araki Y, Imahori H. Quinoxaline-fused porphyrins for dye-sensitized solar cells. *Journal of Physical Chemistry C* 2008;112:4396–405.
- [14] Campbell WM, Jolley KW, Wagner P, Wagner K, Walsh PJ, Gordon KC, et al. Highly efficient porphyrin sensitizers for dye-sensitized solar cells. *Journal of Physical Chemistry C* 2007;111:11760–2.
- [15] Li G, Jiang KJ, Li YF, Li SL, Yang LM. Efficient structural modification of triphenylamine-based organic dyes for dye-sensitized solar cells. *Journal of Physical Chemistry C* 2008;112:11591–9.
- [16] Koumura N, Wang Z, Mori S, Miyashita M, Suzuki E, Hara K. Alkylfunctionalized organic dyes for efficient molecular photovoltaics. *Journal of the American Chemical Society* 2006;128:14256–7.
- [17] Hagberg DP, Edvinsson T, Marinado T, Boschloo G, Hagfeldt A, Sun L. A novel organic chromophore for dye-sensitized nanostructured solar cells. *Chemical Communications* 2006;21:2245–7.
- [18] Li G, Jiang K, Bao P, Li Y, Li S, Yang L. Molecular design of triarylamine-based organic dyes for efficient dye-sensitized solar cells. *New Journal of Chemistry* 2009;33:868–76.
- [19] Wang Z, Koumura N, Cui Y, Takahashi M, Sekiguchi H, Mori A, et al. Hexylthiophene-functionalized carbazole dyes for efficient molecular photovoltaics: tuning of solar-cell performance by structural modification. *Chemistry of Materials* 2008;20:3993–4003.
- [20] Nazeeruddin MK, Humphry-Baker R, Grätzel M, Murrer BA. Efficient near IR sensitization of nanocrystalline TiO₂ films by ruthenium phthalocyanines. *Chemical Communications* 1998;6:719–20.
- [21] Kamat PV, Haria M, Hotchandani S. C₆₀ Cluster as an electron shuttle in a Ru(II)-polypyridyl sensitizer-based photochemical solar cell. *Journal of Physical Chemistry B* 2004;108:5166–70.
- [22] (a) Imahori H, Hayashi S, Hayashi H, Oguro A, Eu S, Umeyama T, et al. Effects of porphyrin substituents and adsorption conditions on photovoltaic properties of porphyrin-sensitized TiO₂ cells. *Journal of Physical Chemistry C* 2009;113:18406–13; (b) Eu S, Hayashi S, Umeyama T, Oguro A, Kawasaki M, Kadota N, et al. Effects of 5-membered heteroaromatic spacers on structures of porphyrin films and photovoltaic properties of porphyrin-sensitized TiO₂ cells. *Journal of Physical Chemistry C* 2007;111:3528–37.